Multibeamlet focusing of intense negative ion beams by an aperture displacement technique

doi: 10.1063/1.1146091

Multibeamlet focusing of intense negative ion beams by an aperture displacement technique

Y. Takeiri,[a] O. Kaneko, Y. Oka, K. Tsumori, E. Asano, R. Akiyama, T. Kawamoto, and T. Kuroda
National Institute for Fusion Science, Nagoya 464-01, Japan

A. Ando
Faculty of Engineering, Tohoku University, Sendai 980-77, Japan

(Received 12 July 1995; accepted for publication 17 August 1995)

Multibeamlet focusing of an intense negative-ion beam has been performed using beamlet steering by aperture displacement. The apertures of the grounded grid were displaced as all 270 beamlets (18×15) in an area of 25 cm×26 cm are steered to a common point (a focal point) in both the two-stage and the single-stage accelerators. The multibeamlets were successfully focused and the *e*-folding half width of 10 cm was achieved 11.2 m downstream from the ion source in both accelerators. The corresponding gross divergence angle is 9 mrad. The negative-ion beamlets are deflected by the electron deflection magnetic field at the extraction grid and the deflection direction reverses line by line, resulting in the beam splitting in the deflection direction. This beamlet deflection was well compensated also using beamlet steering by the aperture displacement of the grounded grid. The beam acceleration properties related to the beam divergence and the H^- ion current were nearly the same for both the two-stage and the single-stage accelerators, and were dependent on the ratio of the extraction to the acceleration electric fields. © *1995 American Institute of Physics.*

I. INTRODUCTION

In next step fusion experimental devices such as ITER (International Thermonuclear Experimental Reactor), a negative-ion-based neutral beam injection (NBI) system is planned,[1] because the neutralization efficiency of negative ions is as high as 60% in the high beam energy range of more than several hundred keV. In order to realize this system much effort has been made to develop high-current and high-energy negative-ion sources.[2–16] Recently more than 10 A of negative-ion current has been obtained[12,14,17–19] and high-energy acceleration to more than 100 keV has been demonstrated.[20–22] The negative-ion current density is, however, much lower than the positive one, and the grid area of the ion source is larger. As a result, the multibeamlet focusing by the steering of individual ion beamlets is required for an efficient injection into the torus plasma.

In the National Institute for Fusion Science, the Large Helical Device (LHD),[23,24] which is the world biggest superconducting helical system, is now under construction, and a 125 keV (*H*)/250 keV (*D*)-20 MW negative-ion-based NBI is planned for the LHD plasma heating.[25] For the LHD–NBI system we have developed large negative-ion sources,[11,13,15–19,22] and obtained 16.2 A of H^- ion current with a current density of 31 mA/cm^2.[18] We have also achieved a high-energy acceleration of 13.6 A of a H^- ion beam to 125 keV.[22] In the LHD-NBI ion source, each grid consists of grid units of 25 cm×25 cm in area, which are jointed with a small angle so that each grid unit would face the same point. With this structure the multibeamlets of negative ions delivered from the ion source can be focused at a common point by the beamlet steering in each grid unit.

Since the negative-ion extraction grid contains permanent magnets for electron suppression, the geometrical shaping of the grid is inapplicable to the multibeamlet focusing in the negative-ion source. On the other hand, the aperture displacement technique for ion beamlet steering is used for multibeamlet focusing in positive-ion sources.[26–30] In the negative-ion source, it is reported that using a single negative-ion beamlet, the steering angle of the beamlet by the aperture displacement was measured and agreed with the prediction of a linear optics theory.[31] Therefore, it is important to demonstrate the multibeamlet focusing of an intense negative-ion beam by the aperture displacement technique.

We have focused the multibeamlets of negative ions delivered from the grid area of 25 cm×26 cm on a common point by aperture displacement of the grounded grid. Moreover, the negative-ion beam deflection by the magnetic field, which is generated by the permanent magnets embedded in the extraction grid, has been compensated also using the beamlet steering by the aperture displacement of the grounded grid. The optimum acceleration conditions of the focused negative-ion beam were investigated for both the two-stage and the single-stage accelerations. In the following, these results are presented in detail.

II. EXPERIMENTAL SETUP

A. External-filter-type large negative-ion source

In multibeamlet focusing experiments, an external-filter-type large negative-ion source was used, which has been developed for the high-energy and high-current negative-ion beam production.[18,22] Figure 1 shows a schematic diagram of the ion source with a two-stage accelerator. The detailed structure is described in Refs. 18 and 22. The dimensions of the arc chamber are 30 cm×62 cm in cross section and 20.6

[a]Electronic mail: takeiri@phlkome.nifs.ac.jp

 0034-6748/95/66(11)/5236/8/$6.00

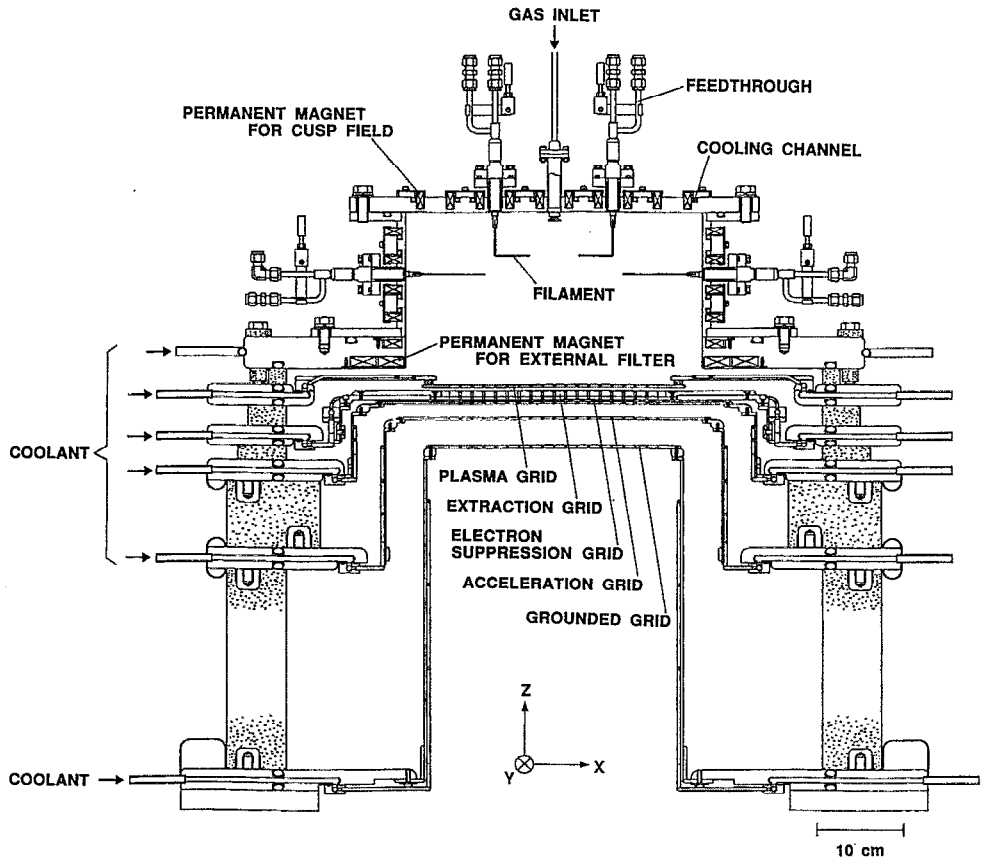

FIG. 1. Schematic diagram of an external-filter-type large negative-ion source with a two-stage accelerator.

cm in depth. The ion source is characterized by a strong external magnetic filter produced by a pair of permanent magnet rows with a separation of 35.4 cm. Two cesium ovens are attached to the side wall of arc chamber. In the two-stage acceleration, there are five grids used—plasma grid (PG), extraction grid (EG), electron suppression grid (SG), acceleration grid (AG), and grounded grid (GG), while three grids, PG, EG, and GG, are used in the single-stage acceleration, as shown in Figs. 2(a) and 2(b), respectively. Although each grid originally has 522 (18×29) apertures in the area of 25 cm×50 cm, the plasma grid made of molybdenum is masked both upward and downward in the longer direction (Y direction in Fig. 1), resulting in 270 (18×15) apertures of 11.3 mm in diameter giving a total area of 25 cm×26 cm. The grounded grid has 270 (18×15) displaced apertures. As shown in Figs. 2(a) and 2(b), the extraction grid contains permanent magnets, which generate the magnetic field suppressing and deflecting the electrons extracted together with the negative ions. With the operation of 522 apertures, the ion source produced 16.2 A of H^- ions, corresponding to 31 mA/cm^2 of the current density at the plasma grid, at the arc efficiency of 0.1 A/kW at the operational gas pressure of 3.8 mTorr in the cesium mode.[18] 13.6 A of H^- ion beam was accelerated to 125 keV in the two-stage acceleration.[22] Thus, this leads us to multibeamlet focusing experiments using intense negative-ion beams. The operational gas pressure was around 3.6 mTorr during the experiments in both the two-stage and the single-stage accelerations.

B. Aperture displacement

The steering of ion beamlets by the aperture displacement has been investigated in the positive-ion sources,[26–30] and is utilized for multibeamlet focusing in the present positive-ion-based NBI system. The theoretical analyses have been performed and compared with the experiments. We have displaced the apertures of the grounded grid, because the steering angle is expected to be proportional to the aperture-displaced amount in both the two-stage and the single-stage accelerations. The negative-ion extraction and acceleration systems are shown in Figs. 2(a) and 2(b) for the two-stage and the single-stage accelerations, respectively. In both cases, the steering angle, θ, is expressed by

$$\theta=(E_{\rm acc}/4W_B)\delta, \tag{1}$$

where δ is the aperture displacement of the grounded grid, $E_{\rm acc}$ the electric field on the upstream side of the grounded grid, and W_B the total beam energy.[30] Here, $E_{\rm acc}$ is defined by the applied voltage divided by the grid gap length [$E_{\rm acc}=V_{\rm acc2}/d_{\rm acc2}$ in Fig. 2(a) and $E_{\rm acc}=V_{\rm acc}/d_{\rm acc}$ in Fig. 2(b)]. Using the focal length of the multibeamlets, f, and the distance of the aperture position from the grid center, x, then $\theta\sim x/f$ and Eq. (1) is modified to

$$\delta/x=4W_B/(E_{\rm acc}f). \tag{2}$$

In the experiments the relative aperture displacements of the grounded grid, δ/x, were 0.0168 for the two-stage accelera-

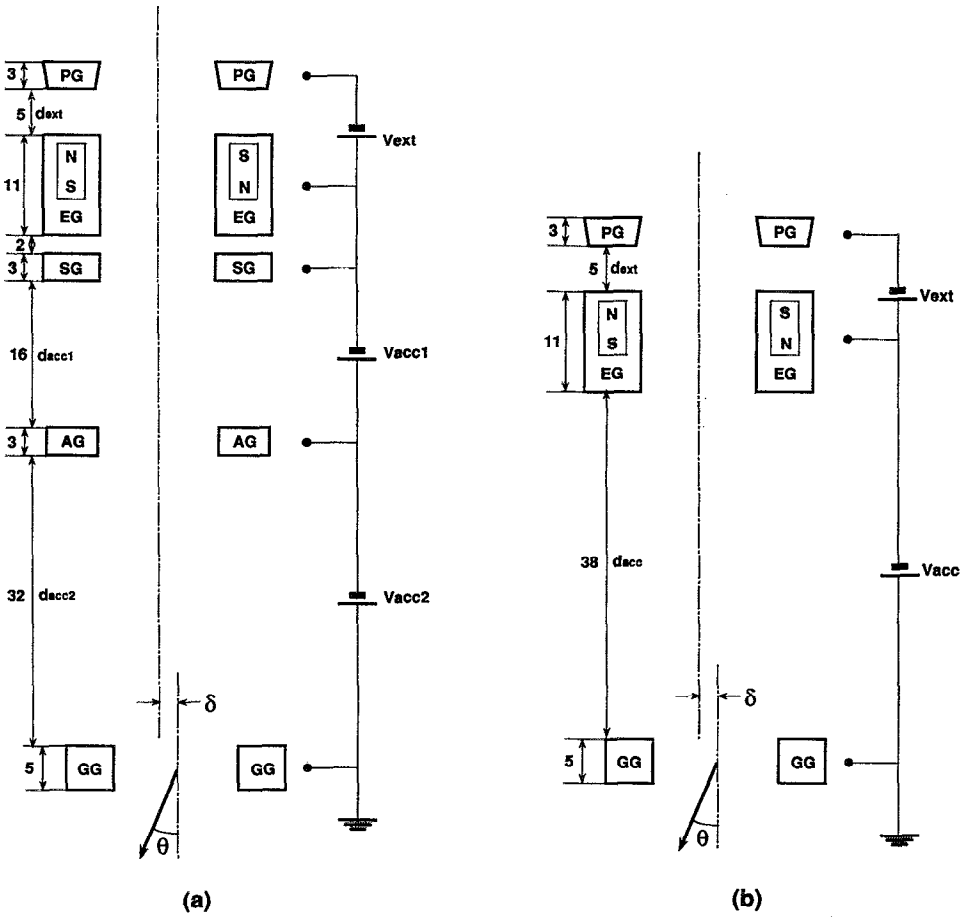

FIG. 2. Grid arrangements along the beam axis and the electrical connections of the power supplies in (a) the two-stage accelerator and (b) the single-stage accelerator. δ is the amount of the displacement and θ the steering angle. S and N denote the polarities of the permanent magnets.

tion and 0.0148 for the single-stage acceleration. Although the focal length varies according to the acceleration condition, it ranged between 11 and 12 m in the experiments.

On the other hand, the negative-ion beam is deflected by the magnetic field generated by the permanent magnets embedded in the extraction grid. As shown in Figs. 2(a) and 2(b), the magnetization direction of the permanent magnets is parallel to the beam axis (Z direction in Fig. 1), and the polarity alternates line by line along the Y (vertical) direction. The directions of the generated magnetic field on both sides of the extraction grid are opposite to each other, and the magnetic field on the plasma grid side extends into the arc chamber. Therefore, the line-integrated transverse magnetic field strength along the beam axis is not zero for the negative-ion beam, resulting in the beamlet deflection in the X (horizontal) direction. Moreover, the deflection direction of the adjacent beamlets in the Y direction is opposite, because the magnetic field direction alternates line by line along the Y direction. Although we will discuss the beam expansion or beam splitting in the X direction by the alternate horizontal beamlet deflection in Sec. III A, the beamlet deflection could be compensated by the aperture displacement technique. In the case of the single-stage acceleration, the amount of the aperture displacement of the grounded grid corresponding to the horizontal steering angle of ± 8 mrad is added to that for the multibeamlet focusing.

C. Negative-ion-based NBI teststand

The ion source is attached to the negative-ion-based NBI teststand[32–35] via a gate valve of 800 mm in diameter. The teststand has two large vacuum chambers, the ion source chamber and the beam dump chamber, connected to each other via a 5-m-long neutralizer with a width of 30 cm. During the experiments a cryopump with a pumping speed of 450 m^3/s was operated in the ion source chamber. Two multichannel calorimeter arrays are installed at the entrance and the exit of the neutralizer, and located 5 and 11.2 m downstream from the ion source, respectively. The calorimeter arrays have 15 channels in the horizontal direction and 25 channels in the vertical direction. The total H^- ion current is estimated using the horizontal and vertical profiles obtained in one shot.

III. EXPERIMENTAL RESULTS

A. Two-stage acceleration

Multibeamlet focusing in the two-stage acceleration was performed using the grid arrangement shown in Fig. 2(a).

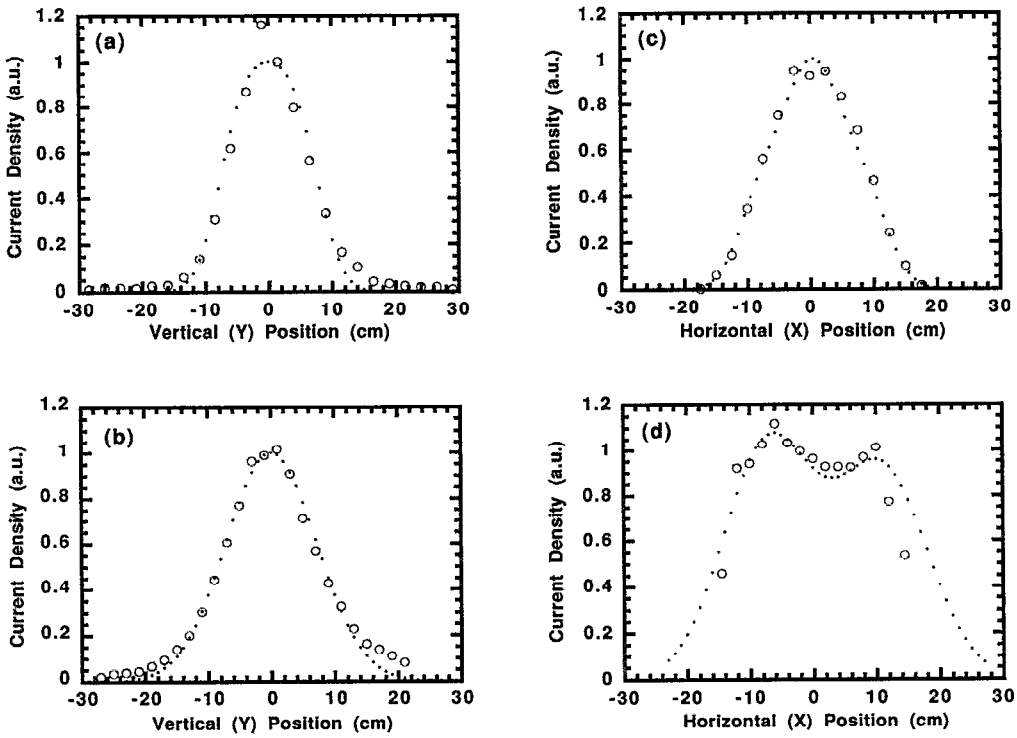

FIG. 3. (a) and (b) vertical (Y) profiles measured by the calorimeter arrays located 5 and 11.2 m downstream from the ion source, respectively, and (c) and (d) the horizontal (X) profiles measured 5 and 11.2 m downstream, respectively, in the two-stage acceleration. The total beam energy is 111 keV, the total H^- ion current 5 m downstream is 3.8 A and the second acceleration voltage is 72 kV. The dotted lines show calculated beam profiles using multigaussian beamlets with a divergence angle of 9 mrad and an alternate horizontal deflection angle of ±8 mrad.

Each aperture of the grounded grid was displaced in order to steer each negative-ion beamlet to a focal point, according to Eq. (2). The focal length changes by the ratio of the first to the second acceleration electric fields, E_{acc1}/E_{acc2}, in the two-stage acceleration from Eq. (2). Therefore, the experimental results presented here were obtained at the constant E_{acc1}/E_{acc2} of around 1, that is equivalent to a single-stage acceleration.

Figures 3(a) and 3(b) show the vertical (Y) profiles measured by the calorimeter arrays 5 and 11.2 m downstream from the ion source, respectively, and Figs. 3(c) and 3(d) show the horizontal (X) profiles measured 5 and 11.2 m downstream, respectively. The total beam energy is 111 keV, the total H^- ion current detected by the calorimeter array 5 m downstream is 3.8 A, and the second acceleration voltage is 72 kV. The focal length is calculated at 11.8 m on this condition. As shown in Figs. 3(a) and 3(b), the vertical profile 5 m downstream is narrow and the vertical profile 11.2 m downstream does not expand, which indicates the gross focusing of the multibeamlets from the area of 25 cm×26 cm. On the other hand, the horizontal profile 5 m downstream is broader, and the horizontal profile 11.2 m downstream is split and the tails on both sides seem to be cut off by the neutralizer walls. Each negative-ion beamlet is deflected horizontally by the magnetic field generated at the extraction grid and the deflection direction alternates line by line in the vertical direction. As a result, the negative-ion beam profile is observed to be split horizontally 11.2 m downstream. We calculated beam profiles using 270 multigaussian beamlets (18×15), each of which has a divergence angle of 9 mrad and the alternate horizontal deflection angle of ±8 mrad. The calculated profiles with a focal length of 11.8 m are also indicated by dotted lines in Figs. 3(a)–3(d). The measured profiles are well fitted to the calculated ones both vertically and horizontally at both calorimeter locations. Thus, the horizontal deflection angle by the magnetic field at the extraction grid is estimated at around 8 mrad at the total beam energy of 111 keV. The gross divergence angle of the negative-ion beam is considered to be 9 mrad.

The optimum beam acceleration condition, meaning the minimum beam divergence angle with the maximum H^- ion current, was investigated by varying the ratio of the first acceleration to the extraction electric fields, E_{acc1}/E_{ext}, keeping the E_{acc1}/E_{acc2} constant. Figure 4(a) shows the FWHMs of the vertical profiles measured 5 and 11.2 m downstream from the ion source as a function of the E_{acc1}/E_{ext}. The arc power is 70 kW and the extraction voltage is 6.2 kV. E_{acc1}/E_{acc2} is constant at 0.93, and the focal length is, then, almost constant, around 11.8 m. At around 1.7 of the E_{acc1}/E_{ext}, the FWHMs show minimums for both the profiles. Although the profile 11.2 m downstream is a little broader than that 5 m downstream, the negative-ion beam is not largely broadened vertically during the transport through the neutralizer, because of the multibeamlet focusing. Figure 4(b) shows the H^- ion current measured with the calorimeter array 5 m downstream, I_{H^-}, and the ratio of the H^- ion current to the second acceleration current, I_{H^-}/I_{acc2}, as a function of the E_{acc1}/E_{ext}. In contrast with the FWHMs observed in Fig. 4(a), the I_{H^-} and the I_{H^-}/I_{acc2} show the maximums at around 1.7 of the E_{acc1}/E_{ext}. Since the focal length

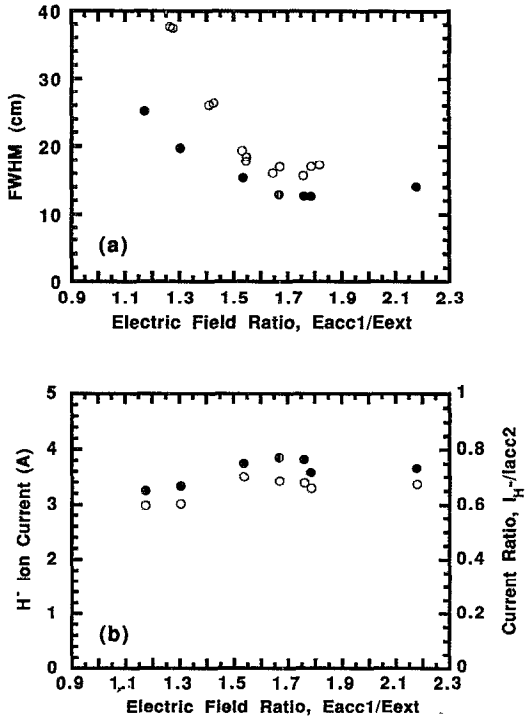

FIG. 4. (a) FWHMs of the vertical profiles measured (●) 5 m and (○) 11.2 m downstream from the ion source, and (b) the H^- ion current (●) and the ratio of the H^- ion current to the second acceleration current, I_{H^-}/I_{acc2} (○), as a function of the ratio of the first acceleration to the extraction electric fields, E_{acc1}/E_{ext}, in two-stage acceleration. The arc power is 70 kW and the extraction voltage is 6.2 kV. The ratio of the first to the second acceleration electric fields, E_{acc1}/E_{acc2}, is constant, 0.93.

is 11.8 m in Fig. 4(a), the *e*-folding half width of the vertical profile measured 11.2 m downstream is considered to correspond approximately to the gross beam divergence. The *e*-folding half width of the vertical profile measured 11.2 m downstream is shown in Fig. 5, as a function of the E_{acc1}/E_{ext}, for the same conditions as those in Fig. 4(a). The corresponding gross divergence angle estimated from the *e*-folding half width is also indicated on the right-hand axis. A gross divergence angle of 9 mrad is achieved, which is

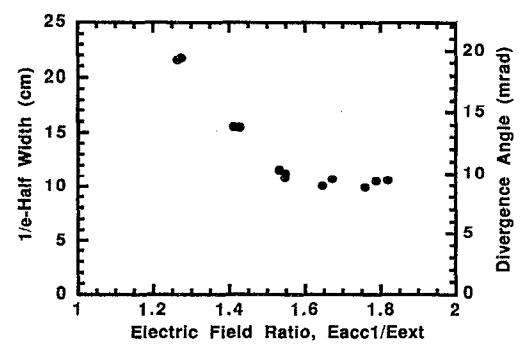

FIG. 5. *e*-folding half width of the vertical profile measured 11.2 m downstream from the ion source as a function of the ratio of the first acceleration to the extraction electric fields, E_{acc1}/E_{ext}, in the two-stage acceleration for the same conditions as those in Fig. 4. The corresponding gross divergence angle estimated from the *e*-folding half width is also indicated on the right-hand axis.

coincident with the results of the profile fitting shown in Fig. 3.

B. Single-stage acceleration

The single-stage acceleration is simpler and more economical than the two-stage acceleration. Since the current density in the negative-ion source is much lower than that in the positive-ion source, the beam expansion due to the space charge during the acceleration could be lower for the negative-ion beam and the single-stage acceleration could be applicable for high-energy acceleration. From the results in the two-stage acceleration, the optimum beam acceleration was achieved by varying the E_{acc1}/E_{ext} with an E_{acc1}/E_{acc2} of about 1, which nearly corresponds to the single-stage acceleration. On the other hand, the electron suppression grid is electrically connected to the extraction grid, and thus, it could be removed. In the experiments in single-stage acceleration, a three-grid system is utilized as shown in Fig. 2(b). The apertures of the grounded grid are displaced in order to gather the individual beamlets at a common point and to compensate the alternate horizontal beamlet deflection by the magnetic field at the extraction grid. The focal length of the multibeamlets is chosen to be around 11.2 m and the alternate horizontal steering angle for compensating the beamlet deflection by the magnetic field is ±8 mrad as determined from the profile fitting in Fig. 3.

The vertical and horizontal profiles measured 5 and 11.2 m downstream from the ion source are shown in Figs. 6(a)–6(d). The extraction voltage is 5.2 kV, the acceleration voltage is 78 kV, and the total H^- ion current estimated with the calorimeter array 5 m downstream is 3.8 A. The calculated profiles using multigaussian beamlets (18×15) with a focal length of 11.2 m and a divergence angle of 9 mrad and with an alternate horizontal deflection angle of ±2 mrad are also indicated by dotted lines in the figures. As shown in Figs. 6(a)–6(d), the profiles are well fitted to the calculated ones. The beam expansion in the horizontal direction by the alternate horizontal beamlet deflection with the magnetic field is not perfectly compensated, and 2 mrad of alternate deflection seems to exist. However, the aperture displacement technique is applicable to the compensation of the alternate beamlet deflection by the magnetic field.

Figure 7(a) shows the *e*-folding half width of the vertical profile measured 11.2 m downstream as a function of the acceleration voltage for the extraction voltages of 5.2, 4.3, and 3.4 kV. The arc power is 60 kW. The divergence angle corresponding to the *e*-folding half width is also indicated on the right-hand axis in the figure. The acceleration voltage giving the minimum divergence becomes higher as the extraction voltage increases. Figure 7(b) shows the total H^- ion current measured 11.2 m downstream, which passes through the neutralizer, as a function of the acceleration voltage for the same extraction voltages as those in Fig. 7(a). Although the acceleration voltage giving the maximum H^- ion current becomes higher as the extraction voltage increases, the maximum H^- ion current for a fixed extraction voltage increases as the extraction voltage increases. This is because the extraction voltages of 4.3 and 3.4 kV are too low to extract fully the negative ions produced at an arc power of 60 kW.

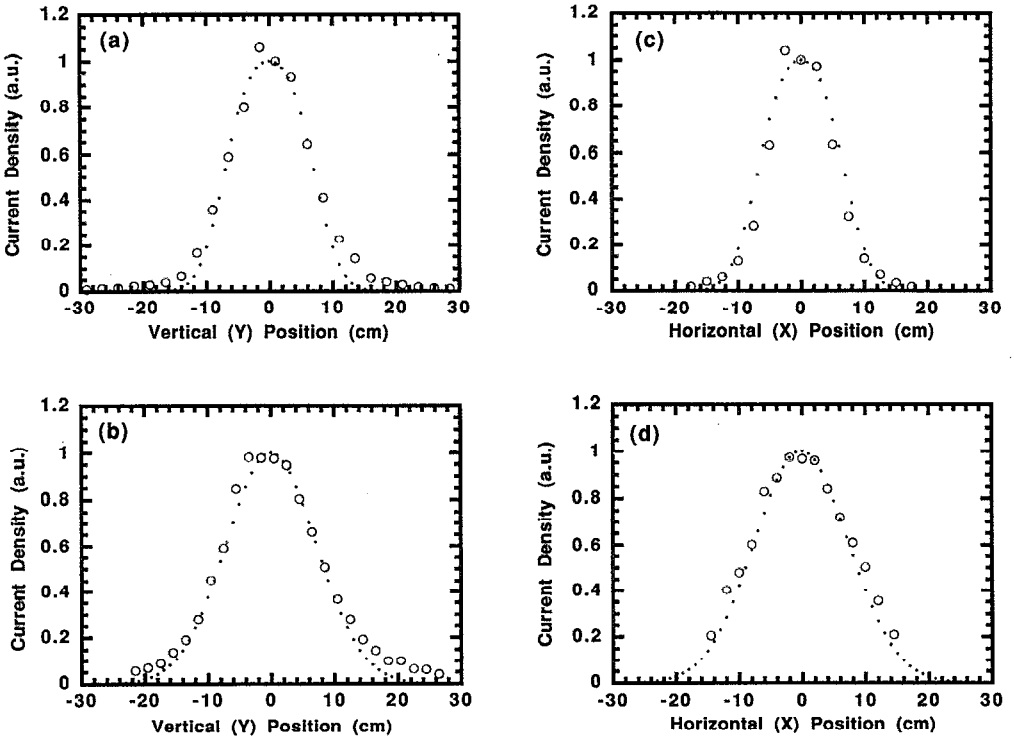

FIG. 6. (a) and (b) vertical (Y) profiles measured 5 and 11.2 m downstream from the ion source, respectively, and (c) and (d) the horizontal (X) profiles measured 5 and 11.2 m downstream, respectively, in the single-stage acceleration. The total beam energy is 83 keV, the total H^- ion current 5 m downstream is 3.8 A and the acceleration voltage is 78 kV. The dotted lines show calculated beam profiles using multigaussian beamlets with a divergence angle of 9 mrad and an alternate horizontal deflection angle of ± 2 mrad.

As shown in Figs. 7(a) and 7(b), the acceleration voltage giving the minimum divergence is a little higher than that giving the maximum H^- ion current.

The ratio of the acceleration to the extraction electric fields, E_{acc}/E_{ext}, has an influence on the beam properties. Figures 8(a) and 8(b) show the e-folding half width of the vertical profile and the total H^- ion current measured 11.2 m downstream, respectively, as a function of the E_{acc}/E_{ext}. The arc powers are 60 kW for the extraction voltages of 5.2, 4.3, and 3.4 kV and 35 kW for the extraction voltages of 4.4 and 3.6 kV. The corresponding divergence angle is also indicated on the right-hand axis in Fig. 8(a). It is recognized that the dependency of the e-folding half width on the E_{acc}/E_{ext} is nearly the same for the various combinations of the extraction voltage and the arc power, as well as that of the H^- ion current. The minimum divergence angles are nearly the same for the different arc powers, at which the negative-ion currents are different. Although the E_{acc}/E_{ext} giving the minimum divergence is a little higher than that giving the maximum H^- ion current, these dependencies on the E_{acc}/E_{ext} are relatively broad. Thus, in the single-stage acceleration the ion source should be operated in the condition for the maximum H^- ion current due to the high acceleration efficiency.

Although the electron suppression grid is removed in the single-stage acceleration, no increase of the current ratio of the acceleration current to the H^- ion current, I_{acc}/I_{H^-}, i.e., no increase of the accelerated electron current, is observed.

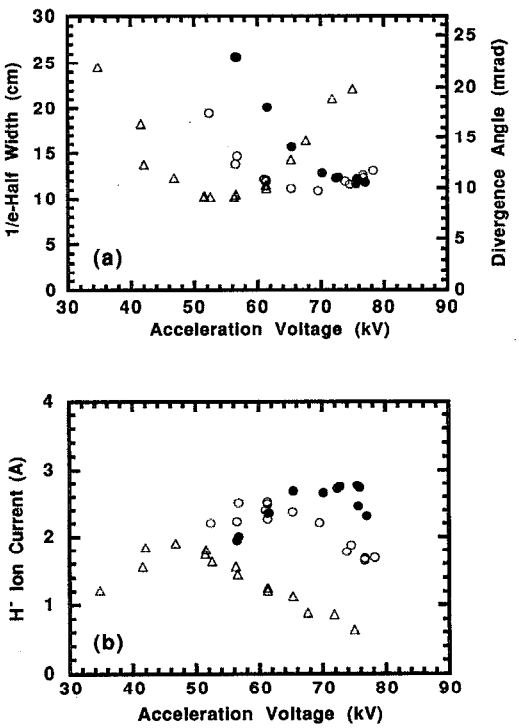

FIG. 7. (a) e-folding half width of the vertical profiles 11.2 m downstream and (b) the total H^- ion currents measured 11.2 m downstream, in the single-stage acceleration as a function of the acceleration voltage for the extraction voltages of (●) 5.2, (○) 4.3, and (△) 3.4 kV. The gross divergence angle corresponding to the e-folding half width is also indicated on the right-hand axis in (a). The arc power is 60 kW.

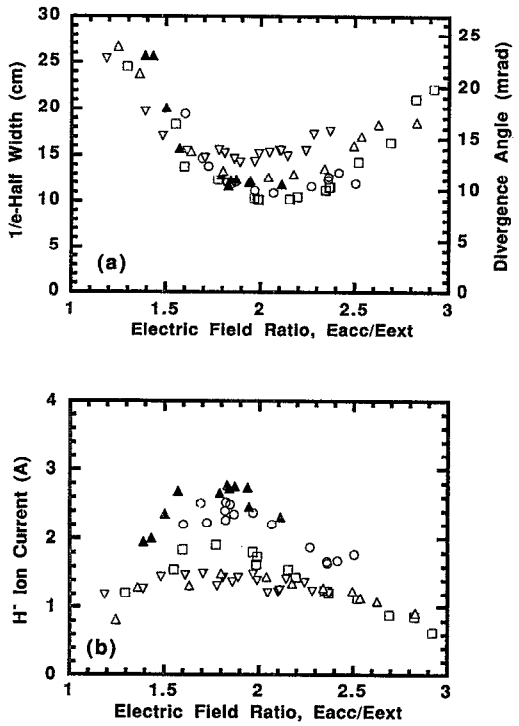

FIG. 8. (a) e-folding half width of the vertical profiles and (b) the total H^- ion current both measured 11.2 m downstream in the single-stage acceleration, as a function of the ratio of the acceleration to the extraction electric fields, E_{acc}/E_{ext}, for the extraction voltages, V_{ext}, of (▲) 5.2, (○) 4.3, and (□) 3.4 kV at an arc power P_{arc} of 60 kW and a V_{ext} of (▽) 4.4 and (△) 3.6 kV at a P_{arc} of 35 kW. The divergence angle corresponding to the e-folding half width is also indicated on the right-hand axis in (a).

IV. DISCUSSIONS

The multibeamlets of the negative-ion beam are successfully focused by the aperture displacement technique. In both the two-stage and the single-stage accelerations the aperture displacement of the grounded grid is effective for the beamlet steering, because a linear correlation between the amount of the displacement and the steering angle is simple as indicated in Eq. (1) and the steering angle is not largely dependent on the total beam energy. The alternate horizontal deflection of the negative-ion beamlets by the magnetic field at the extraction grid is compensated also by the aperture displacement technique. The line-integrated transverse magnetic field strength generated by the embedded permanent magnets in the extraction grid, $\int B\,dz$, is 200–300 G cm along the beam axis, depending on the negative-ion emitting surface. The corresponding beamlet deflection angle, θ_m, is approximately estimated at 4–7 mrad at a beam energy of 100 keV from a simple equation,

$$\theta_m = \sqrt{e/2MV}\int B\,dz, \tag{3}$$

where M is the ion mass, V the total acceleration voltage, and e the electron charge. The deflection angle determined by profile fitting in Figs. 3(a)–3(d) is 8 mrad, suggesting that the negative-ion emitting surface could be extruded toward the extraction grid. Detailed experiments using a single beamlet are required for the relation between the deflection angle and the emitting surface position. In the case of single-stage acceleration, the aperture displacement for the alternate beamlet steering angle of ±8 mrad is added to that for the multibeamlet focusing. As shown in Figs. 6(a)–6(d), the deflection angle of 2 mrad is not compensated, because the total beam energy in Fig. 6 is lower than that in Fig. 3. The deflection angle by the magnetic field is dependent on the square root of the total energy, and the deflection angle in Fig. 6 is calculated to be larger by about 1.2 mrad than that in Fig. 3. Therefore, the beamlet deflection by the magnetic field is considered to be well compensated by the aperture displacement technique. However, it is noted that the beamlet steering angle due to aperture displacement is independent of the beam energy, while the beamlet deflection angle due to the magnetic field is dependent on it. In an actual injector, the beam energy is varied less than 40%, and the deflection angle changes by 1–2 mrad at most. The accuracy of the aperture displacement also has an influence on the steering angle. In the case of the single-stage acceleration shown in Fig. 2(b), the steering angle changes by 0.6 mrad when the amount of the displacement deviates by 0.1 mm. The deviation of the displacement is caused by the fabrication accuracy and the thermal expansion of the grid, and the changes in the individual steering angles result in the aberration of the multibeamlet focusing. However, since a displacement accuracy of 0.1 mm is possible, this aberration would hardly cause serious problems.

In conclusion the multibeamlet focusing of an intense negative-ion beam is achieved with a gross divergence angle of 9 mrad using the aperture displacement technique, which can also be used to compensate the beamlet deflection by the magnetic field generated at the extraction grid. These results enable the intense negative ion beam to be transported a long distance.

[1] T. Nagashima, R. S. Hemsworth, M. Makowski, D. Remsen, and the ITER Joint Central Team and Home Teams, Proc. of the 15th Int. Conf. on Plasma Physics and Controlled Nuclear Fusion Research, Seville, Spain, 1994 (IAEA, Vienna), IAEA-CN-60/E-P-9 (to be published).
[2] M. Bacal, G. W. Hamilton, A. M. Bruneteau, H. J. Doucet, and J. Taillet, Rev. Sci. Instrum. **50**, 719 (1979).
[3] K. N. Leung, K. W. Ehlers, and M. Bacal, Rev. Sci. Instrum. **54**, 56 (1983).
[4] R. L. York, Ralph R. Stevens, Jr., K. N. Leung, and K. W. Ehlers, Rev. Sci. Instrum. **55**, 681 (1984).
[5] M. Bacal, A. H. Bruneteau, and M. Nachman, J. Appl. Phys. **55**, 15 (1984).
[6] A. J. T. Holmes, G. Dammerts, and T. S. Green, Rev. Sci. Instrum. **56**, 1697 (1985).
[7] Y. Okumura, H. Horiike, T. Inoue, T. Kurashima, S. Matsuda, Y. Ohara, and S. Tanaka, *Proceedings of the 4th International Symposium on Production and Neutralization of Negative Ions and Beams*, Upton, NY, 1986 (AIP, New York, 1986), AIP Conf. Proc. No. 158, p. 309.
[8] A. J. T. Holmes, L. M. Lea, A. F. Newman, and M. P. S. Nightingale, Rev. Sci. Instrum. **58**, 223 (1987).
[9] K. N. Leung, K. W. Ehlers, C. A. Hauck, W. B. Kunkel, and A. F. Lietzke, Rev. Sci. Instrum. **59**, 453 (1988).
[10] M. Hanada, T. Inoue, H. Kojima, Y. Matsuda, Y. Ohara, Y. Okumura, K. Watanabe, and M. Seki, Rev. Sci. Instrum. **61**, 499 (1990).
[11] Y. Takeiri, A. Ando, O. Kaneko, Y. Oka, R. Akiyama, T. Kawamoto, A. Karita, K. Mineo, and T. Kuroda, Proc. of the 16th Symp. on Fusion Technology, London, 1990 (Elsevier, Amsterdam, 1991), p. 1012.
[12] Y. Okumura, M. Hanada, T. Inoue, H. Kojima, Y. Matsuda, Y. Ohara, Y. Oohara, M. Seki, Y. Suzuki, and K. Watanabe, Proc. of the 16th Symp. on Fusion Technology, London, 1990 (Elsevier, Amsterdam, 1991), p. 1026.
[13] A. Ando, Y. Takeiri, K. Tsumori, O. Kaneko, Y. Oka, R. Akiyama, T.

Kawamoto, K. Mineo, K. Kurata, and T. Kuroda, Rev. Sci. Instrum. **63**, 2683 (1992).
[14] Y. Okumura, M. Hanada, T. Inoue, H. Kojima, Y. Matsuda, Y. Ohara, M. Seki, and K. Watanabe, *Proceedings of the 5th International Symposium on the Production and Neutralization of Negative Ions and Beams*, Brookhaven, 1990 (AIP, New York, 1990), AIP Conf. Proc. No. 210, p. 169.
[15] A. Ando, K. Tsumori, Y. Takeiri, O. Kaneko, Y. Oka, T. Okumura, H. Kojima, Y. Yamashita, R. Akiyama, T. Kawamoto, K. Mineo, T. Kurata, and T. Kuroda, *Proceedings of the 6th International Symposium on Production and Neutralization of Negative Ions and Beams*, Upton, NY, 1992 (AIP, New York, 1992), AIP Conf. Proc. No. 287, p. 339.
[16] K. Tsumori, A. Ando, Y. Takeiri, O. Kaneko, Y. Oka, T. Okuyama, H. Kojima, Y. Yamashita, T. Kawamoto, R. Akiyama, and T. Kuroda, Rev. Sci. Instrum. **65**, 1195 (1994).
[17] A. Ando, K. Tsumori, Y. Oka, O. Kaneko, Y. Takeiri, E. Asano, T. Kawamoto, R. Akiyama, and T. Kuroda, Phys. Plasmas **1**, 2813 (1994).
[18] Y. Takeiri, A. Ando, O. Kaneko, Y. Oka, K. Tsumori, R. Akiyama, E. Asano, T. Kawamoto, T. Kuroda, M. Tanaka, and H. Kawakami, Rev. Sci. Instrum. **66**, 2541 (1995).
[19] Y. Takeiri, A. Ando, O. Kaneko, Y. Oka, K. Tsumori, T. Takanashi, R. Akiyama, E. Asano, T. Kawamoto, M. Tanaka, H. Kawakami, T. Okuyama, Y. Suzuki, and T. Kuroda, Proc. of the 18th Symposium on Fusion Technology, Karlsruher, 1994 (Elsevier, Amsterdam, 1995), p. 609.
[20] J. Pamela, M. Fumelli, F. Jequier, A. Simonin, M. Hanada, Y. Okumura, and K. Watanabe, *Proceedings of the 6th International Symposium on Production and Neutralization of Negative Ions and Beams*, Upton, NY, 1992 (AIP, New York, 1992), AIP Conf. Proc. No. 287, p. 695.
[21] K. Miyamoto, M. Hanada, T. Inoue, N. Miyamoto, A. Nagase, Y. Ohara, Y. Okumura, and K. Watanabe, Proc. of the 18th Symposium on Fusion Technology, Karlsruher, 1994 (Elsevier, Amsterdam, 1995), p. 625.
[22] Y. Takeiri, A. Ando, O. Kaneko, Y. Oka, K. Tsumori, R. Akiyama, E. Asano, T. Kawamoto, M. Tanaka, and T. Kuroda, J. Plasma Fusion Res. **71**, 605 (1995).
[23] A. Iiyoshi, Proc. of the 13th Symp. on Fusion Engineering, Knoxville, 1989 (IEEE, New York, 1990), p. 1007.
[24] A. Iiyoshi, M. Fujiwara, O. Motojima, N. Ohyabu, and K. Yamazaki, Fusion Technol. **17**, 169 (1990).
[25] Y. Takeiri, O. Kaneko, F. Sano, A. Ando, Y. Oka, K. Hanatani, T. Obiki, and T. Kuroda, Proc. of the first Int. Toki Conf. on Plasma Physics and Controlled Nuclear Fusion, Toki, Japan, 1989 (National Institute for Fusion Science, Nagoya, Japan, 1989), p. 272.
[26] L. D. Stewart, J. Kim, and S. Matsuda, Rev. Sci. Instrum. **46**, 1193 (1975).
[27] J. R. Coupland and T. S. Green, Nucl. Instrum. Methods **125**, 197 (1975).
[28] W. L. Gardner, J. Kim, M. M. Menon, and J. H. Whealton, Rev. Sci. Instrum. **49**, 1214 (1978).
[29] J. R. Conrad, Rev. Sci. Instrum. **51**, 418 (1980).
[30] Y. Okumura, Y. Mizutani, and Y. Ohara, Rev. Sci. Instrum. **51**, 471 (1980).
[31] T. Inoue, M. Hanada, M. Mizuno, Y. Ohara, Y. Okumura, Y. Suzuki, M. Tanaka, and K. Watanabe, *Proceedings of the 6th International Symposium on Production and Neutralization of Negative Ions and Beams*, Upton, NY, 1992 (AIP, New York, 1992), AIP Conf. Proc. No. 287, p. 316.
[32] Y. Oka, A. Ando, O. Kaneko, Y. Takeiri, K. Tsumori, R. Akiyama, T. Kawamoto, K. Mineo, T. Kurata, and T. Kuroda, Proc. of the 14th Symp. on Fusion Engineering, San Diego, 1991 (IEEE, New York, 1992), p. 70.
[33] O. Kaneko, A. Ando, Y. Oka, Y. Takeiri, K. Tsumori, R. Akiyama, T. Kawamoto, T. Kurata, K. Mineo, and T. Kuroda, Proc. of the 17th Symp. on Fusion Technology, Rome, 1992 (Elsevier, Amsterdam, 1993), p. 544.
[34] Y. Takeiri, A. Ando, O. Kaneko, Y. Oka, K. Tsumori, R. Akiyama, T. Kawamoto, and T. Kuroda, *Proceedings of the 6th International Symposium on Production and Neutralization of Negative Ions and Beams*, Upton, NY, 1992 (AIP, New York, 1992), AIP Conf. Proc. No. 287, p. 869.
[35] Y. Takeiri, Y. Oka, O. Kaneko, A. Ando, K. Tsumori, R. Akiyama, T. Kawamoto, and T. Kuroda, Rev. Sci. Instrum. **65**, 1198 (1994).